Fluorescence Studies on Modes of Cytochalasin B and Phallotoxin Action on Cytoplasmic Streaming in *Chara*

EUGENE A. NOTHNAGEL, LARRY S. BARAK, JOSEPH W. SANGER, and W. W. WEBB
School of Applied and Engineering Physics and Department of Physics, Cornell University, Ithaca, New York 14853; and Department of Anatomy, School of Medicine, University of Pennsylvania, Philadelphia, Pennsylvania 19174

ABSTRACT Various investigations have suggested that cytoplasmic streaming in characean algae is driven by interaction between subcortical actin bundles and endoplasmic myosin. To further test this hypothesis, we have perfused cytotoxic actin-binding drugs and fluorescent actin labels into the cytoplasm of streaming *Chara* cells. Confirming earlier work, we find that cytochalasin B (CB) reversibly inhibits streaming. In direct contrast to earlier investigators, who have found phalloidin to be a potent inhibitor of movement in amoeba, slime mold, and fibroblastic cells, we find that phalloidin does not inhibit streaming in *Chara* but does modify the inhibitory effect of CB. Use of two fluorescent actin probes, fluorescein isothiocyanate-heavy meromyosin (FITC-HMM) and nitrobenzoxadiazole-phallacidin (NBD-Ph), has permitted visualization of the effects of CB and phalloidin on the actin bundles. FITC-HMM labeling in perfused but nonstreaming cells has revealed a previously unobserved alteration of the actin bundles by CB. Phalloidin alone does not perceptibly alter the actin bundles but does block the alteration by CB if applied as a pretreatment. NBD-Ph perfused into the cytoplasm of streaming cells stains actin bundles without inhibiting streaming. NBD-Ph staining of actin bundles is not initially observed in cells inhibited by CB but does appear simultaneously with the recovery of streaming as CB leaks from the cells. The observations reported here are consistent with the established effects of phallotoxins and CB on actin in vitro and support the hypothesis that streaming is generated by actin-myosin interactions.

The highly organized cytoplasmic streaming exhibited by the giant internodal cells of characean algae has long made these cells an attractive system for the study of cell motility (4). Accumulated evidence has suggested that motility in a variety of eukaryotic cells is actomyosin-dependent (21). Measurements of streaming-velocity profiles in characean cells have suggested that the motive force is generated primarily at the interface between the stationary ectoplasm and motile endoplasm (17). Early ultrastructural studies have revealed the presence of microfilament bundles attached to the chloroplasts at this interface (26). Subsequent electron and, more recently, fluorescence microscope studies using labeling by heavy meromyosin (20, 27, 29) or antiactin antibodies (45) have demonstrated the presence of actin in these subcortical microfilament bundles and established the unidirectional orientation of the actin filaments (19). Other light microscope studies have suggested the presence of endoplasmic filaments that appeared to branch from the subcortical actin bundles and participate in the generation of the motive force (1, 2).

The demonstration of actin in characean cells has encouraged workers to search for evidence of myosin in these cells as well. Using a perfusion technique that permitted manipulation of internal pH and ion and ATP concentrations, Williamson observed the ATP-dependent motion of endoplasmic organelles along the subcortical actin bundles (41). These observations, together with recent ultrastructural studies (3, 5, 24, 44), suggest that myosinlike molecules may be present on the surface of these motile organelles. Biochemical extraction of *Nitella* myosin has been reported (18), but its association with motile organelles has not been demonstrated. Nevertheless, it is now widely assumed that actin and myosin work together to produce cytoplasmic streaming in characean algae (42).

Another method of probing microfilament-dependent cell motility is to examine the effects of actin-binding drugs. A number of workers have examined the effect of cytochalasins on cytoplasmic streaming in characean algae (10, 13, 25, 40, 41). Cytochalasin B (CB) has been found to cause essentially complete inhibition of streaming, although the concentrations

THE JOURNAL OF CELL BIOLOGY · VOLUME 88 FEBRUARY 1981 364-372

of CB required (2–100 μM) are generally somewhat higher than those required for inhibition of motility and disruption of microfilaments in other cell types (37). Because the subcortical actin bundles are thought to be an essential part of the streaming mechanism, it might be expected that inhibition of streaming by CB should also disrupt the ultrastructure of these bundles. In fact, however, this disruption has generally not been observed (10, 13, 25, 40). Only a CB effect on the attachment of actin bundles to the cortex in rhizoid cells has been reported (13). No such effect has been reported for internodal cells. Other reported structural effects of CB on characean algae include an increase in the number of minivacuoles in the cytoplasm (40), an inhibition of ATP-induced extraction of endoplasmic filaments from perfused cells (41, 44), and a reduction in the affinity of endoplasmic organelles for subcortical actin bundles (41). Recently, it has been reported that CB stabilizes subcortical actin bundles against extraction by perfusion with a disruptive low-ionic-strength solution (43).

The actin-specific phallotoxins, notably phalloidin and phallacidin, exhibit strong binding to F-actin, promote actin polymerization, and stabilize F-actin against strong agents such as 0.6 M KI, DNase I, and cytochalasins (38). Unlike CB, these bi-cyclic peptides are generally not membrane permeable (32, 35, 36, 38). However, upon microinjection, phalloidin inhibits cytoplasmic streaming and causes ultrastructural disruption in *Amoeba proteus* and *Physarum polycephalum* (32, 36) and interferes with locomotion of fibroblastic cells (35). A recent report suggests that phalloidin applied in the extracellular medium stops streaming in *Allium*, *Chara*, and *Nitella* (28), while another report finds no inhibition of streaming in *Vaucheria* (8).

In preliminary reports we have described the synthesis and characterization of a fluorescent derivative of phallacidin (6, 7) and demonstrated its use in the fluorescent labeling of actin bundles in *Chara* without the inhibition of cytoplasmic streaming (7). In the present paper we describe in further detail the effects of cytochalasin B and phallotoxins on streaming and actin bundle structure in *Chara*. We confirm the inhibition of cytoplasmic streaming by CB and demonstrate that phallotoxins applied at high concentrations inside perfused cells do not inhibit streaming but, in fact, accelerate recovery of streaming after inhibition by CB. Using fluorescent heavy meromyosin from muscle as a label for subcortical actin bundles, we find no disruption of bundle structure by phalloidin but rather demonstrate a previously unobserved alteration of the bundles by CB. Using fluorescent phallacidin as an actin label, we have studied fluorescence-labeled subcortical actin bundles during active streaming and also during the recovery of streaming after inhibition by CB. The results of these experiments are interpreted in terms of established in vitro effects of phallotoxins on actin (38) and in terms of the recently reported findings regarding the effects of cytochalasins on actin polymerization (11, 12, 15, 22).

MATERIALS AND METHODS

Growth and Preparation of Chara Cells

Chara corallina Klein ex Willd., en R. D. W. (=*C. australis* R.Br.) was laboratory grown in plastic garbage cans. The plants were rooted in soil and covered with modified Forsberg medium (14). Internodal cells 4–8 cm in length were isolated from the plants and placed in petri dishes containing artificial pond water (APW; 1 mM NaCl, 0.1 mM KCl, 0.1 mM $CaCl_2$, 1 mM morpholinepropanesulfonic acid, pH 7.2) at least 24 h before the start of an experiment.

To facilitate fluorescence microscope viewing, "windows" through the dense chloroplast layer were produced by a modification of the technique of Kamitsubo (16). Windows 100 μm in diameter were produced by spot irradiating cells in petri dishes for 40 s with ~30 W/cm^2 of 476-nm laser light. Under these conditions all chloroplasts disappear from the windows within 24 h after irradiation. To allow sufficient time for repair of the subcortical actin bundles in the windows, cells were incubated for another 7–10 d in APW before they were used in fluorescence-labeling experiments.

Chemicals

Ordinary laboratory chemicals were standard reagent grade. CB was obtained from Sigma Chemical Co., St. Louis, Mo. Four different lots of phalloidin were obtained from Boehringer Mannheim Biochemicals, Indianapolis, Ind. Other phalloidin was purified by column chromatography from a mixture of mushroom toxins residual to an amanitin purification by Yocum (46). All supplies of phalloidin showed characteristic ultraviolet absorption, ~95% purity as estimated from thin-layer chromatography, and identical biological activity.

Fluorescein isothiocyanate–rabbit heavy meromyosin (FITC-HMM) was prepared and stored as described previously (30). Immediately before use FITC-HMM was transferred to the desired buffer by gel filtration on Sephadex G-25.

7-Nitrobenz-2-oxa-1,3-diazole-phallacidin (NBD-Ph) was prepared as described previously (6, 7) and stored at −20°C in anhydrous methanol. Aliquots of NBD-Ph in methanol were dried by a jet of nitrogen gas and were dissolved in the appropriate buffer for use.

Application of Drugs to Intact Cells

In experiments testing the effects of CB or phallotoxins on intact cells, the drugs were applied simply by immersing the intact cells in APW that contained the drug to be tested. Phallotoxins were dissolved directly in APW. In these and all other CB experiments reported in this paper, CB was taken from a 10 mM CB in dimethylsulfoxide (DMSO) stock solution and added to the appropriate buffer. In all cases, the final DMSO concentration in the buffer was 1% (vol/vol) or less. In control experiments in which 1% DMSO was applied either outside or inside the cells, we found no effect of DMSO on cytoplasmic streaming, FITC-HMM labeling, or NBD-Ph labeling.

Introduction of Drugs and Fluorescent Labels into Cells by Perfusion

Phalloidin, NBD-Ph, and CB were introduced directly into the interior of cells through use of the vacuolar perfusion technique described in detail by Tazawa et al. (33). The essential steps in this perfusion technique are as follows: (*a*) The internodal cell is removed from medium (APW), blotted dry, and placed on a small plastic operating table. A drop of perfusion fluid is added at each end of the cell. (*b*) At the first signs of turgor collapse, the ends of the cell are cut off, and one end of the operating table is elevated slightly so as to produce a gentle flow of the perfusion fluid through the vacuole. (*c*) As soon as the vacuolar sap is fully replaced by perfusion fluid, excess fluid is blotted away and the ends of the cell are ligated. (*d*) Partial turgor pressure is restored by covering the perfused cell with 200 mM sorbitol solution. A second ligation, closer to the center of the cell than the first, is then performed at each end of the cell. (*e*) The perfusion operation is now complete, and the cell is returned to medium (APW), where it regains full turgor pressure.

In our hands the entire perfusion operation requires ~7 min. In experiments examining the time-course of streaming after perfusion, time (t) = 0 min was defined as the time at which perfusion was completed, i.e., the time at which the perfused cell was returned to APW. Tazawa's perfusion fluid (TPF), as used in the experiments reported here, consisted of 30 mM HEPES, 5 mM EGTA, 6 mM $MgCl_2$, 1 mM ATP, 23.5 mM methanesulfonic acid, and 250 mM sorbitol (pH = 7.0, as adjusted with KOH). Phalloidin and NBD-Ph were dissolved directly in TPF, whereas CB was added from the 10 mM DMSO stock solution.

In experiments involving FITC-HMM labeling, the fluorescent label was introduced into the cell by the perfusion technique of Williamson (41), modified only by the substitution of TPF in place of the perfusion fluid described by Williamson. Williamson's technique (41) differs effectively from Tazawa's technique (33) in that a higher rate of perfusion is used, thus sweeping away most of the endoplasm as well as the vacuolar sap, and in that the ends of the cell are not ligated after perfusion.

Measurement of the Rate of Cytoplasmic Streaming

Measurement of cytoplasmic streaming rates was accomplished by combining

stopwatch timing with microscope observation through a calibrated eyepiece. For each data point the rate of streaming was sampled at a number of locations in the cell, and the rate recorded was the fastest speed observed in the cell at the indicated time.

Probably reflecting the relative success of individual perfusion operations, the rate and persistence of streaming in perfused cells showed considerable cell-to-cell variability. After cells were perfused with TPF, for example, streaming persisted for times ranging from 1 to 3 h. Because of this large variability, curves presented here showing the time-course of streaming in perfused cells represent data averaged for six to nine different cells. Error bars shown on these curves are standard deviations arising from individual variations within the cell population rather than from measurement precision limitations. In contrast to perfusion experiments, experiments testing the effects of drugs on intact cells revealed relatively little (usually <20%) cell-to-cell variability. Hence each curve presented here showing the time-course of streaming in intact cells represents data averaged for just two different cells.

Fluorescence Microscopy and Photography

Fluorescence microscopy was carried out by use of either blue excitation light from a mercury lamp or 476-nm light from a krypton ion laser. Red chloroplast autofluorescence was blocked by use of our special liquid barrier filter as described previously (27). Images of FITC-HMM fluorescence were recorded directly on Kodak Tri-X film. Images of NBD-Ph fluorescence were recorded on Kodak Tri-X film after intensification by a NVC-100 image intensifier (NI-TEC, Inc., Niles, Ill.). Film negatives were scanned with a Joyce Mark III C microdensitometer (Joyce, Loebl & Co., Ltd., Gateshead, England). The response of the photographic film as exposed in the microscope was determined by recording a sequence of equal-time exposures over a range of light levels measured by the microscope photometer. The characteristic film curve thus obtained was used to convert scans of fluorescent bundle images from density to corrected linear exposure.

RESULTS

Effects of Drugs on Streaming in Intact Cells

Cytoplasmic streaming in intact *Chara* cells was strongly inhibited by the presence of 50 μM CB in the extracellular medium (Fig. 1). The rate of streaming dropped by 30% within 10 min of the application of CB and approached full inhibition within 90 min. On the other hand, Fig. 1 also shows that 1 mM phalloidin in the extracellular medium caused no change in cytoplasmic streaming over 150 min. We have applied 1 mM phalloidin in the extracellular medium of *Chara* continuously for 72 h, after which cells still showed normal appearance and vigorous streaming (results not shown). Preincubation of intact cells for 150 min in 1 mM phalloidin had no effect on the inhibition of streaming by 50 μM CB (Fig. 1).

Effects of Drugs on Streaming in Perfused Cells

Because phallotoxins are not membrane permeable for many cell types (32, 35, 36, 38), the effects of these drugs can be tested reliably only when the drugs are introduced directly into the cytoplasm. We have used the perfusion technique of Tazawa et al. (33) to introduce drugs into the interior of *Chara* cells. Although only the vacuolar sap is replaced during the perfusion, the EGTA in the perfusion fluid (TPF) causes dissolution of the tonoplast within 10–20 min after the cell is returned to APW at the completion of perfusion (33), so that chemicals dissolved in the TPF then become directly available in the cytoplasm.

Fig. 2 confirms the earlier work of Tazawa et al. (33) and shows that cells perfused by this technique typically recovered streaming to >50% of the preperfusion rate within 10 min and then continued streaming for >100 min.

Streaming in cells perfused with TPF containing either phalloidin at 1 mM or the fluorescence-labeled phallotoxin NBD-Ph at 30 μM was not significantly different from streaming in cells perfused with TPF alone (Fig. 2). Higher concentrations of NBD-Ph were not tested.

Perfusion with TPF containing 100 μM CB produced 100% inhibition of streaming <2 min after perfusion (Fig. 3). Streaming began a slow recovery 25–35 min later and accelerated to 25% of the preperfusion rate at ~80 min. This recovery was seen first as slow movements in the endoplasm located within a few cell diameters of the ends of the cell. It was usually 10–

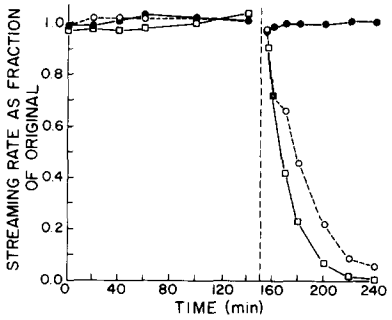

FIGURE 1 Effect on streaming of drugs applied in the bathing medium of intact cells. At t = 0 min, cells were placed in APW (closed circles and open circles) or in 1 mM phalloidin in APW (open squares). At t = 150 min, the bathing medium was changed to APW containing 1% DMSO (closed circles), 50 μM CB, and 1% DMSO (open circles), or 50 μM CB, 0.67 mM phalloidin, and 1% DMSO (open squares). Average original streaming rates were 82 (closed circles), 83 (open circles), and 77 μm/s (open squares).

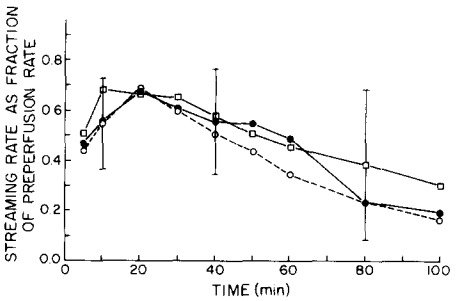

FIGURE 2 Effect on streaming of phallotoxins applied intracellularly by Tazawa's perfusion technique. Perfusion was completed at t = 0 min. Cells were perfused with TPF (closed circles), 1 mM phalloidin in TPF (open circles), or 30 μM NBD-Ph in TPF (open squares). Average preperfusion streaming rates were 78 (closed circles), 87 (open circles), and 91 μm/s (open squares). Error bars are drawn symmetrically about the corresponding data points and represent standard deviations.

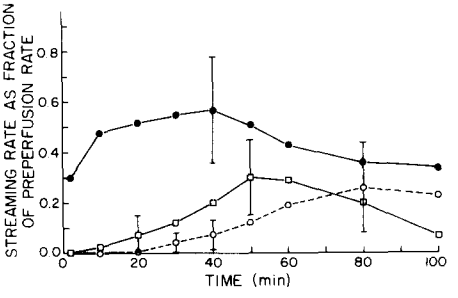

FIGURE 3 Effect on streaming of drugs applied intracellularly by Tazawa's perfusion technique. Perfusion was completed at t = 0 min. Cells were perfused with TPF containing 1% DMSO (closed circles), 100 μM CB, and 1% DMSO (open circles), or 100 μM CB, 1 mM phalloidin, and 1% DMSO (open squares). Average preperfusion streaming rates were 90 (closed circles), 81 (open circles) and 81 μm/s (open squares). Error bars are drawn symmetrically about the corresponding data points and represent standard deviations.

15 min later before similar movements could be observed in the endoplasm located near the middle of the same cell (results not shown).

Perfusion with TPF containing both 100 μM CB and 1 mM phalloidin likewise produced full inhibition of streaming within 2 min (Fig. 3). In these cells, however, streaming began a slow recovery only 10–15 min later and by 50 min had accelerated to 30% of the preperfusion rate.

The Distribution of Actin Bundles as Visualized by FITC-HMM Labeling

Cells were treated with drugs and labeled with FITC-HMM through a sequence of perfusions of the type described by Williamson (41). The particular sequence of perfusion solutions and time durations used for each experiment is given in the accompanying figure captions. It is to be noted that these perfused cells (Figs. 4 and 5) differ from intact streaming cells in two significant aspects. First, these perfusions were carried out using ATP-free TPF (TPF less ATP) to obtain FITC-HMM binding. ATP is required for streaming (41), however, so the cells as shown in Figs. 4 and 5 were not streaming. Second, much of the endoplasm is swept out of cells during perfusion by the Williamson technique (41). Because the cells of Figs. 4 and 5 were each perfused several times during the course of labeling and rinsing, these cells became essentially devoid of endoplasm.

Cells perfused with FITC-HMM in the absence of ATP showed heavily labeled filament bundles (Fig. 4 *a* and *b*). If cells were perfused with FITC-HMM in the presence of 10 mM ATP, filament bundles labeled so weakly that images on film negatives appeared only dimly, if at all. Control cells perfused with FITC-antimouse IgG fraction or with free fluorescein showed no fluorescent bundles (results not shown). Because of the thick layer of bound FITC-HMM, actin bundles in labeled cells were often large enough to be visualized by bright-field microscopy as well as by fluorescence microscopy (results not shown). Bundles in intact cells or in perfused but unlabeled cells were rarely visible by bright-field microscopy. Chloroplast fluorescence appearing in Figs. 4 and 5 is not FITC-HMM fluorescence but yellow autofluorescence induced by prolonged illumination (27).

The distribution of FITC-HMM-labeled actin bundles in window areas was studied 7–10 d after window formation and compared (to the extent permitted by the optical interference from the chloroplasts) with the distribution of bundles under intact chloroplasts. Examination of window areas revealed a layer of labeled bundles ~1–3 μm inside the plasma membrane (Fig. 4 *a*). This was the location of the new ectoplasm-endoplasm interface within the pocket region left vacant by removal of the chloroplasts. About 7 μm closer to the center of the cell, another layer of labeled bundles was found at the same level as the endoplasmic face of the chloroplasts at the edge of the window (Fig. 4 *b*). These inner bundles spanned the open pocket region of the window area and, at the edges of the window, merged directly into the intact subcortical actin bundle layer attached to the endoplasmic face of the chloroplasts. This merging was most easily observed along the lateral edges of the windows (Fig. 5 *c*). By focusing up and down between the two layers of bundles (Fig. 4 *a* and *b*), it could be seen that bundles in the outer layer (Fig. 4 *a*), upon reaching the edges of the pocket region, generally turned inward and also merged with the intact layer of subcortical actin bundles.

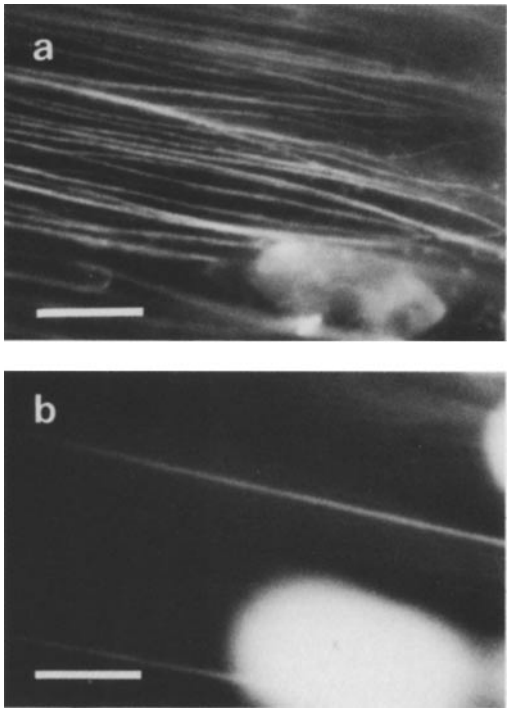

FIGURE 4 FITC-HMM labeling of actin bundles in a chloroplast window in *Chara*. Labeling was accomplished by Williamson-type perfusions that left the cell essentially devoid of endoplasm. Perfusion sequence: 15 min with TPF; 3 min with ATP-free TPF (TPF less ATP); 20 min with 0.57 mg/ml FITC-HMM in TPF less ATP; 5 min with TPF less ATP. (*a*) Fluorescence micrograph with plane of focus slightly inside the plasma membrane. (*b*) Fluorescence micrograph of the same field as in *a* but with plane of focus 7 μm closer to the center of the cell. Bars, 10 μm.

When compared with subcortical actin bundles attached to intact chloroplasts, the bundles in the outer layer (Fig. 4 *a*) were more frequently branched or frayed and hence appeared smaller in size but greater (about two times) in number. In contrast, the bundles in the inner layer (Fig. 4 *b*) were somewhat fewer in number than subcortical actin bundles in intact areas. A few of these inner bundles appeared exceptionally large, apparently because of lateral aggregation of two or three subcortical actin bundles in the span across the pocket region (Fig. 5 *a*).

The apparent division of the subcortical actin bundle layer into two spatially separated layers, outer (Fig. 4 *a*) and inner (Fig. 4 *b*), was observed only in window areas. Intact areas without windows showed FITC-HMM staining on only a single layer of subcortical bundles attached to the chloroplasts. Hence this apparent division of the subcortical bundles into layers can be regarded as an artifact associated with window formation. The inner layer of bundles (Fig. 4 *b*), being located at the same level as subcortical bundles attached to chloroplasts and appearing more intact (not branched or frayed), was judged to be more like a native layer of subcortical actin bundles than was the outer layer of bundles (Fig. 4 *a*). Thus, subsequent micrographs (Figs. 5–7) are focused on only those bundles found in the inner layer, i.e., bundles similar to those shown in Fig. 4 *b*.

To test whether FITC-HMM-labeled actin bundles were capable of transverse motions, we perfused labeled cells at high flow rates (~1 cm/s) first in one direction and then in the other. Observation of the fluorescent actin bundles during this perfusion reversal revealed that actin bundles in the inner layer

(e.g., Fig. 4*b*) did not swing around during flow reversal and were capable of only very small (≤1 μm) transverse motions. Actin bundles in the outer layer (e.g., Fig. 4*a*) showed no detectable motion during these perfusions.

Effects of Drugs on the Appearance of Subcortical Actin Bundles as Visualized by FITC-HMM Labeling

Cells pretreated for 30 min with 1 mM phalloidin and then labeled with FITC-HMM in the presence of phalloidin contained fluorescent actin bundles (Fig. 5*a*) that could not be distinguished from bundles in control cells not treated with phalloidin. (Cf. Fig. 4*b*; note that this micrograph does not precisely illustrate the control treatment because the fluorescent bundles of Fig. 4*b* were partially photobleached during the prior photographic exposure of Fig. 4*a*. Examination of many bundles in several cells revealed no significant difference between control and phalloidin-treated bundles.)

Cells pretreated for 30 min with 100 μM CB and then labeled with FITC-HMM in the presence of CB contained fluorescent actin bundles (Fig. 5*b*) that appeared diminished compared to those in control cells. The intensity of bundle staining was sufficiently low that it was necessary to decrease the printing time for Fig. 5*b* to one-fifth the time used for Fig. 5*a* and *c*. When an attempt was made to print the negative for Fig. 5*b* at the same exposure as used for Fig. 5*a* and *c*, the fluorescent bundles disappeared into the black background. Original film negatives for Fig. 5*a–c* were all exposed and processed under identical conditions. In some CB-treated cells, aggregates of intensely staining material occasionally appeared in association with the bundles (see arrows in Fig. 5*b*).

The effect of this CB treatment on actin bundles in perfused cells was further characterized by microdensitometric scanning of the negative film images of the FITC-HMM-labeled bundles. Six film negatives from two different CB-treated cells were scanned as were six film negatives from control (no CB) cells. After background subtraction, the average peak height exposure measured on CB-treated bundles was 18 ± 8% of that measured on control bundles. The full-width at half-height of CB-treated bundles was 0.40 ± 0.05 μm, whereas the corresponding width of control bundles was 0.64 ± 0.12 μm. The term "diminished" will be used to describe CB-treated bundles that show these combined reductions in FITC-HMM staining intensity and apparent width.

Cells pretreated for 30 min with 1 mM phalloidin, another 30 min with 1 mM phalloidin and 100 μM CB contained fluorescent actin bundles that appeared indistinguishable from actin bundles in cells not treated with CB (Fig. 5*c*). No aggregates of brightly staining material were observed.

NBD-Ph Labeling of Actin Bundles in Actively Streaming Chara

Intact *Chara* rhizoids (more optically transparent than internodes) immersed for 10 h in APW containing 30 μM NBD-Ph showed vigorous cytoplasmic streaming but no evidence suggesting internalization of the fluorescent marker.

To introduce NBD-Ph into the cytoplasm, we perfused internodes by the Tazawa technique (33) with TPF containing NBD-Ph. Preliminary experiments revealed that the quality of staining observed was quite sensitive to NBD-Ph concentration, with the optimal level being ~30 μM. At higher concentrations, staining of the actin bundles was obscured by diffuse background fluorescence because of excess NBD-Ph in the endoplasmic/vacuolar and ectoplasmic regions. At concentrations <30 μM, bundle staining was weak and comparable in intensity to a diffuse, variable autofluorescence that appeared to arise

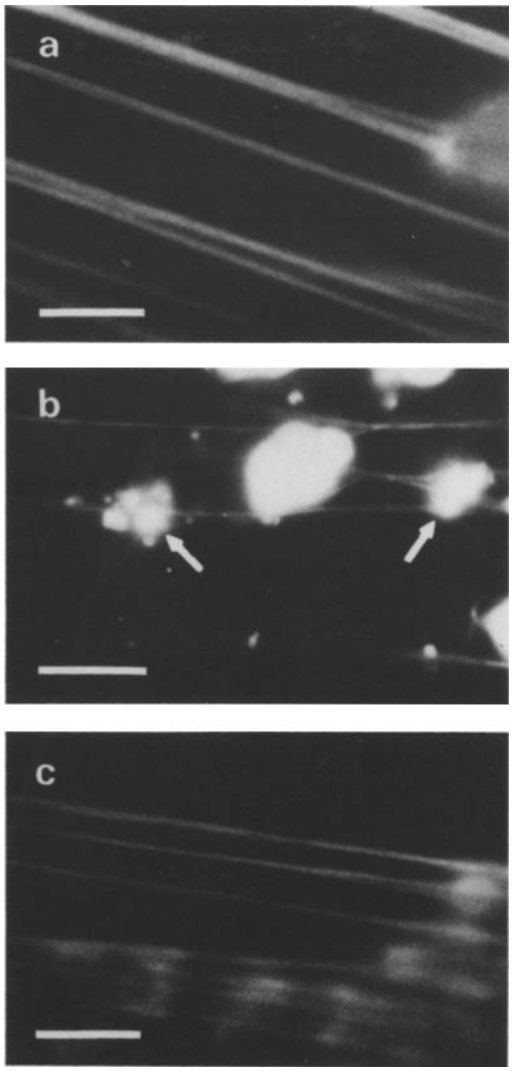

FIGURE 5 Fluorescence micrographs of FITC-HMM labeling of drug-treated subcortical actin bundles in windows in *Chara*. Drugs were applied by Williamson-type perfusions that left the cells essentially devoid of endoplasm. (*a*) Phalloidin-treated actin bundles. The exceptionally large bundles appear to be lateral aggregates of several ordinary bundles. Aggregation is also observed in control cells and is not dependent upon drug treatment. Perfusion sequence: 30 min with 1 mM phalloidin in TPF; 1 min with TPF less ATP; 20 min with 1 mM phalloidin and 0.43 mg/ml FITC-HMM in TPF less ATP; 5 min with 1 mM phalloidin in TPF less ATP. (*b*) CB-treated actin bundles. Arrows indicate aggregates of FITC-HMM stained material. The print exposure time used for this micrograph was one-fifth that used for *a* and *c*. See text. Perfusion sequence: 30 min with 100 μM CB and 1% DMSO in TPF; 1 min with 100 μM CB and 1% DMSO in TPF less ATP; 20 min with 100 μM CB, 1% DMSO, and 0.43 mg/ml FITC-HMM in TPF less ATP; 5 min with 100 μM CB and 1% DMSO in TPF less ATP. (*c*) Phalloidin-pretreated, CB- and phalloidin-treated actin bundles. Perfusion sequence: 30 min with 1 mM phalloidin in TPF; 30 min with 1 mM phalloidin, 100 μM CB, and 1% DMSO in TPF; 1 min with 100 μM CB and 1% DMSO in TPF less ATP; 20 min with 1 mM phalloidin, 100 μM CB, 1% DMSO, and 0.43 mg/ml FITC-HMM in TPF less ATP; 5 min with 1 mM phalloidin, 100 μM CB, and 1% DMSO in TPF less ATP. Bars, 10 μm.

primarily from the cell wall in chloroplast-free windows.

Fig. 6*a* shows fluorescence-stained actin bundles in a cell perfused with TPF containing 30 μM NBD-Ph. This micrograph was recorded 35 min after perfusion, at which time the cell was still very actively streaming at ~74 μm/s. NBD-Ph-labeled actin bundles in streaming cells generally exhibited no or only small (≤1 μm) transverse motions. <1% of the fluorescent bundles observed did, however, exhibit larger undulations of ~5 μm amplitude. In contrast to results obtained with FITC-HMM staining, staining with NBD-Ph did not increase the bright-field visibility of the actin bundles.

The specificity of NBD-Ph binding to actin bundles was tested by perfusing cells with TPF containing both 30 μM NBD-Ph and 2 mM phalloidin. Cells perfused in this manner showed no fluorescent actin bundles (Fig. 6*b*) but did show diffuse fluorescence in the endoplasmic/vacuolar and ectoplasmic regions. Cells perfused with NBD-chloride and NBD-ethanolamine also showed only diffuse fluorescence and no fluorescent actin bundles (results not shown).

NBD-Ph Staining in Cells Recovering from CB-induced Streaming Inhibition

To follow actin bundles during recovery of streaming in CB-treated cells, we perfused cells with TPF containing both 100 μM CB and 30 μM NBD-Ph. This concentration of NBD-Ph was high enough to allow visualization of the actin bundles but was low enough to avoid the acceleration of the rate of recovery found at 1 mM phalloidin (Fig. 3).

Fig. 7*a* is a fluorescence micrograph recorded through a window located near the middle of a cell that had been perfused

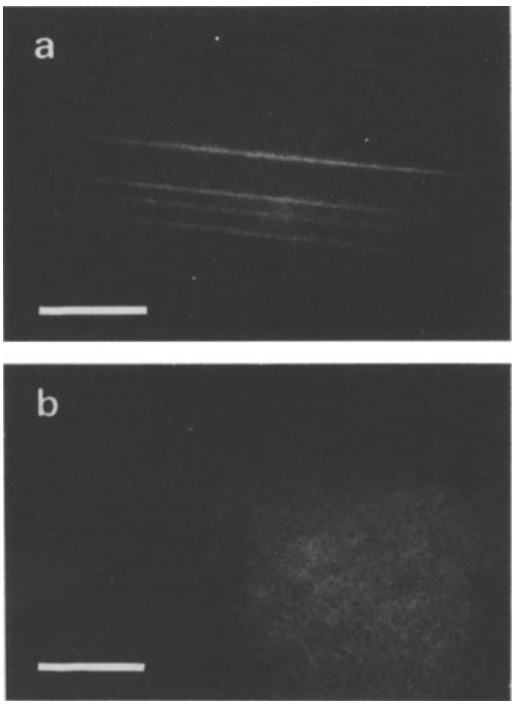

FIGURE 6 NBD-Ph labeling of subcortical actin bundles in chloroplast windows in streaming *Chara*. Fluorescence micrographs showing competitive labeling. (*a*) Cell perfused by Tazawa technique with TPF containing 30 μM NBD-Ph. Micrograph recorded 35 min after completion of perfusion. (*b*) Cell perfused by Tazawa technique with TPF containing 30 μM NBD-Ph and 2 mM phalloidin. Micrograph recorded 33 min after completion of perfusion. Bars, 10 μm.

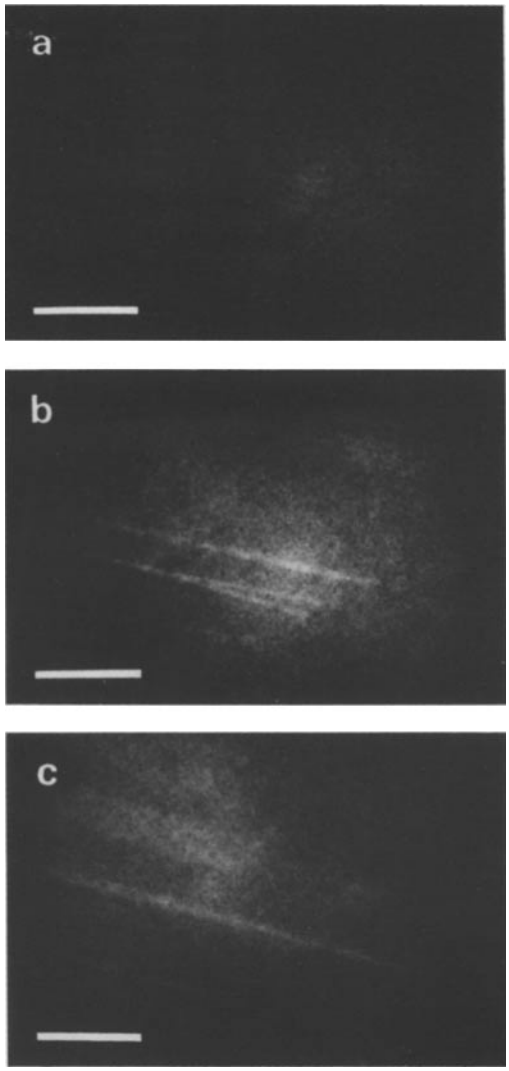

FIGURE 7 Fluorescence micrographs demonstrating delayed NBD-Ph staining of subcortical actin bundles in cells inhibited by CB. (*a*) Cell perfused by Tazawa technique with TPF containing 30 μM NBD-Ph, 100 μM CB, and 1% DMSO. Window area near middle of cell at 49 min after completion of perfusion. Local streaming rate ≤1 μm/s. No labeled bundles were visible in any plane of focus. (*b*) Same cell and field as in *a*, 55 min after completion of perfusion. Local streaming rate = 8 μm/s. NBD-Ph labeled bundles are now visible. (*c*) Control cell perfused by Tazawa technique with TPF containing 30 μM NBD-Ph and 1% DMSO. Window area 26 min after completion of perfusion. Streaming rate = 67 μm/s throughout the cell. NBD-Ph labeled bundles are already visible. Bars, 10 μm.

49 min earlier with TPF containing both CB and NBD-Ph. Streaming in the area had just begun slow recovery after CB inhibition and was ≤1 μm/s. No fluorescent actin bundles were visible in any plane of focus. Fig. 7*b* shows the same field 55 min after perfusion, by which time the local streaming rate had recovered to 8 μm/s and NBD-Ph labeling had begun to appear on the actin bundles.

This simultaneous recovery of streaming and development of NBD-Ph staining of actin bundles could be observed more than once in a single cell having several windows through the chloroplast layer. The resumption of streaming and onset of fluorescent staining of bundles could be seen first in windows located within a few cell diameters of the ends of a cell at t = 30–40 min after perfusion. After first observing this simulta-

neous pair of events near an end of a cell, we found that rapid refocusing on a window near the middle of the cell allowed observation of the simultaneous onset of streaming and staining of actin bundles again after an additional 5–15 min had elapsed.

For comparison, the time-course of NBD-Ph staining of actin bundles was studied in cells perfused with 30 μM NBD-Ph but no CB. These cells showed prompt recovery of rapid streaming throughout the cell (Fig. 2), and then later, at ~20–23 min after perfusion, NBD-Ph labeled bundles appeared dimly above background (Fig. 7 *c*). By 30 min after perfusion, the labeling reached maximum intensity. Labeling developed uniformly throughout the cells, i.e., labeled actin bundles did not appear in windows near ends of cells sooner than in windows near the middle of cells.

DISCUSSION

This work began with an examination of the effects of extracellularly applied CB and/or phalloidin on cytoplasmic streaming in *Chara corallina*. Confirming earlier results (10, 13, 25, 40), strong inhibition of cytoplasmic streaming by 50 μM CB was observed (Fig. 1). In apparent disagreement with a recent report (28), no evidence was found to suggest that extracellularly applied phalloidin has any influence on cytoplasmic streaming, even when the drug is applied at 1 mM concentration for several days.

Because many cell types lack rapid plasma membrane permeability for phallotoxins (32, 35, 36, 38), streaming was also studied in *Chara* cells where CB and/or phallotoxins were applied intracellularly by perfusion techniques. These experiments showed that CB applied intracellularly at 100 μM stops streaming <2 min after perfusion (Fig. 3). Recovery from this inhibition begins within 25–35 min, probably because of leakage of CB from the cell. This recovery occurs first near the ends of the cell and later in the middle, presumably because CB molecules near an end can escape through both the sides and the ends.

No inhibition of cytoplasmic streaming could be produced with 1 mM phalloidin applied intracellularly even during experiments continuing for several hours (Fig. 2). That phalloidin is active in *Chara* and that it does enter the cell via perfusion are indicated by the result of perfusion with both 1 mM phalloidin and 100 μM CB together. In this case, streaming stops, as with CB perfusion alone, but recovery of streaming is accelerated by ~20 min (Fig. 3). Moreover, perfusion with fluorescence-labeled phallotoxin, NBD-Ph, stains cytoplasmic bundles (Fig. 6 *a*). Addition of 2 mM phalloidin together with 30 μM NBD-Ph prevents staining of the bundles although a diffuse (nonspecific?) background fluorescence remains.

As expected, both NBD-Ph and FITC-HMM stain subcortical bundles resembling those found in other studies to contain unidirectional actin filaments (19, 20, 27, 29, 45). Fluorescence-stained actin bundles are most clearly observed in windows through the chloroplast layer. However, FITC-HMM staining of these bundles has revealed that window formation is often accompanied by an apparent artifact, the separation of the subcortical actin bundles into two distinct layers. A new outer layer of bundles (Fig. 4 *a*) appears within the pocket formed by removal of the chloroplasts. The inner layer of bundles (Fig. 4 *b*) appears unperturbed but may have lost some bundles to the outer layer formed in the pocket. Photon correlation experiments have shown that longitudinal and transverse streaming velocities are not measurably altered by window formation (31), so it seems that any alteration of streaming by this separation of bundles into layers was too small to measure. Nevertheless, this artifact must be kept in mind when interpreting micrographs showing bundles or filaments in chloroplast windows. Earlier reports (1, 2) have included Nomarski interference micrographs showing fibrillar structures in chloroplast windows of *Nitella* cells in which streaming had been transiently stopped. The fibrillar structures reported there appear morphologically identical to the fluorescent actin bundles shown in Fig. 4 *a* and *b*. The earlier studies reported that these fibrillar structures exhibited large (~5 μm) undulations during streaming, although direct observation of these undulations could be achieved only in exceptional cases (1, 2). In the present study, only a few (<1%) of the NBD-Ph-labeled bundles in streaming cells were found to be capable of transverse motions comparable to those described previously (1, 2). The present work cannot rule out the suggestion that these undulations generate streaming (1, 2), but the alternative suggestion that these are merely passive undulations of broken bundles (20) can also not be ruled out.

Fluorescence labeling of actin bundles was used in experiments examining the mechanism of action of actin-binding drugs in *Chara*. The results presented here show that CB applied in sufficient dosage (30-min preincubation at 100 μM) causes actin bundles to appear diminished in FITC-HMM fluorescence in cells perfused with a solution (TPF) that would, if not for the presence of CB, support streaming. Aggregates of fluorescent material sometimes associated with bundles (Fig. 5 *b*) may be comparable to the aggregates of actin observed in CB-treated fibroblastic cells (34). Microdensitometer measurements on photographic images of the CB-treated, FITC-HMM-stained actin bundles revealed that the diminished appearance arises from both a reduction in fluorescence staining intensity and a reduction in the apparent width of the bundles. The apparent widths of labeled CB-treated bundles (0.40 ± 0.05 μm) and labeled control bundles (0.64 ± 0.12 μm) are both greater than the 0.2-μm width usually reported for unlabeled bundles (2). The larger apparent widths of the bundles as observed here by fluorescence microscopy may be attributed to the thick layer of bound FITC-HMM and to the limited theoretical resolving power (0.26 μm) of the objective lens used to record the fluorescent images.

Inhibition of streaming by CB precedes the diminished appearance of the bundles shown in Fig. 5 *b*. Total inhibition of streaming occurs within 2 min after perfusion with 100 μM CB (Fig. 3), whereas the diminished appearance shown in Fig. 5 *b* occurs only after 30-min preincubation with 100 μM CB. Less change in bundle appearance was observed at preincubation time <30 min, and extrapolation to 2 min suggests that visible effects on the bundles would be negligible at the time when streaming is stopped. A conjecture about the mechanism that diminishes the actin bundles is suggested by some of the following experiments.

Use of the fluorescent actin probe NBD-Ph in perfused, streaming cells has permitted more direct investigations of the mechanism of CB inhibition of streaming in *Chara*. Unlike FITC-HMM, NBD-Ph can be used under conditions that permit streaming so that fluorescence staining and CB-inhibition experiments can be conducted simultaneously in the same cell.

When cells are perfused with 100 μM CB together with 30 μM NBD-Ph, no labeling of actin bundles is seen before active streaming begins (Fig. 7 *a*) but labeling does appear simulta-

neously with the recovery of streaming (Fig. 7 *b*). These observations do not necessarily imply, however, that actin bundles are absent from cells during CB inhibition. Because 30 μM NBD-Ph normally stains the actin bundles to an intensity that is only slightly greater than that of the diffuse background, any circumstance that significantly impairs the binding of NBD-Ph to the bundles can be expected to prevent the detection of bundle staining above the background intensity. Such a circumstance could arise if NBD-Ph were in some way prevented from reaching the vicinity of the actin bundles or, alternatively, if NBD-Ph reached the actin bundles as usual but binding to the bundles were in some way impaired.

The experiments reported here show that phalloidin by itself does not alter either cytoplasmic streaming (Fig. 2) or the visible properties of actin bundles (Fig. 5 *a*). It does, however, modify both the CB inhibition of streaming (Fig. 3) and the CB-diminished appearance of FITC-HMM-labeled actin bundles (Fig. 5 *c*). In contrast, the effect of microinjected phalloidin in amoeba (32, 36) and 3T3 cells (35) is complete inhibition of movement and in *Physarum* (32) is complete, irreversible cessation of streaming in the area of microinjection. The results reported here for *Chara* are similar to the results recently reported by Blatt et al. (8), who found that phalloidin alone had no direct effect on streaming in the alga *Vaucheria* but did protect against CB inhibition of streaming. In *Vaucheria*, however, phalloidin is apparently able to cross the plasma membrane, as these effects were observed with extracellularly applied drugs (8).

These marked differences in response to phalloidin suggest that there are significant differences between the molecular mechanisms driving streaming in *Chara* and *Vaucheria* and the mechanisms driving streaming and movement in *Amoeba*, *Physarum*, and fibroblastic cells. If phalloidin acts in vivo as it does in vitro to promote actin polymerization and prevent depolymerization (15, 23, 38), then the failure of phalloidin to inhibit streaming implies that cyclic polymerization/depolymerization of actin, thought to be a necessary part of motility in some systems (21, 35, 36), is not a necessary step in the generation of cytoplasmic streaming in *Chara*. In the case of *Amoeba* and fibroblasts, the entire cell must be able to move and, with this translocation, change the distribution of actin. *Physarum*, a syncytium, grows outward and must be able to integrate the actin in the old areas with the actin in the new areas. In contrast to *Amoeba*, fibroblast, and *Physarum* cells, the internodal cells of *Chara* do not actively change their position. Once the cell has reached its full size, there is no need to alter its actin bundles. The insensitivity of *Chara* to phallotoxins would therefore be a reflection of the long-term stability of the actin polymer bundles used for cytoplasmic streaming.

The observations presented here, taken together with the established effects of phallotoxins (38, 39) and cytochalasins (11, 12, 15, 22) on actin in vitro, suggest a hypothesis for the mode of CB inhibition of cytoplasmic streaming in characean algae. We propose that CB inhibits streaming by causing a net release of actin monomers and/or oligomers from the subcortical actin bundles into the endoplasm. The force-generating interaction between the presumptive endoplasmic myosin and the subcortical actin bundles may be competitively inhibited by this same released actin. Interaction between the presumptive endoplasmic myosin and free actin monomers (9) and/or oligomers could not itself generate the organized, directed force required to drive streaming. This mechanism inhibits streaming without gross disruption of the subcortical actin bundles. It only requires release of some actin monomers and/or oligomers that may leave the subcortical actin bundles for the most part quite intact. Prolonged exposure (30 min) to CB during perfusion would lead to the continuous release and removal of more actin and thus to the appearance of a diminished bundle system long after streaming is stopped (Fig. 5 *b*).

The proposed CB-induced net release of actin monomers and/or oligomers from the subcortical bundles might be achieved by various mechanisms. If there normally occurs even a very low level of actin cycling between depolymerized and polymerized forms in *Chara*, then CB may cause a net release of actin from the subcortical bundles by blocking the readdition of monomer actin to the bundles (11, 12, 22). Alternatively, CB may attack the surface filaments of subcortical actin bundles, causing breaks (15) and releasing actin monomers and/or oligomers by a more direct mechanism.

Just as the in vitro destabilization of F-actin by CB (11, 12, 15, 22) is inhibited by phalloidin (15, 23), so too *Chara* actin bundles seem to be protected in cells preincubated with phalloidin and then treated with CB and phalloidin (Figs. 5 *b* and *c*). When CB and phalloidin are added together to *Chara* cells, however, streaming is totally inhibited initially (Fig. 3). We attribute this to faster penetration of CB through the tonoplast. The perfusion technique used in these experiments requires 10–20 min before tonoplast dissolution occurs (33) and begins to allow passage of substances such as phalloidin to which the cell is not normally permeable. CB, which can enter the intact *Chara* cell, would, therefore, reach actin filaments much faster than phalloidin. The resumption of streaming that is accelerated by phalloidin occurs at approximately the time when tonoplast dissolution should allow entry of phalloidin into the cytoplasm, i.e., 10 min after perfusion (Fig. 3). Subsequently, phalloidin may speed repolymerization of the actin that was disrupted by CB and thereby also accelerate the recovery of streaming.

The hypothesis that CB inhibits streaming by releasing actin monomers and/or oligomers into the *Chara* endoplasm suggests an interpretation of the observed simultaneous recovery of streaming and appearance of labeled bundles in cells perfused with both CB and NBD-Ph (Fig. 7). In addition to competitively inhibiting streaming, released actin may also impair the binding of NBD-Ph to the actin bundles by polymerizing in the presence of NBD-Ph to form short soluble filaments that bind and divert NBD-Ph away from the bundles. Because actin polymerized in the presence of phallotoxin will bind about six times as much phallotoxin as will prepolymerized actin (39), released actin may be especially effective in binding NBD-Ph.

The proposed hypothesis for the mechanism of CB inhibition of streaming implies that the streaming endoplasm of characean algae normally contains only very low levels of free G-actin. This result is consistent with the observation that streaming is not inhibited by phalloidin (Fig. 2) and also suggests a partial test of the hypothesis itself: perfusion of *Chara* with exogenous actin should induce at least a transient inhibition of streaming. These experiments are now in progress.

The results of experiments presented here are consistent with the hypothesis that cytoplasmic streaming in characean algae is driven by an interaction between subcortical actin bundles and a presumptive endoplasmic myosin. Results obtained with phallotoxins and CB emphasize the importance of the actin component of the system. The presumptive endoplasmic myosin component requires further investigation.

We are indebted to R. Rogers Yocum for his gifts of phallacidin and phalloidin and to Roger M. Spanswick for supplying us with starting cultures of *Chara*. We are pleased to acknowledge discussions with W. R. Briggs, Mike Frish, J. M. Sanger, and K. Weber, and wish to express special gratitude to Masashi Tazawa for his demonstration of the perfusion technique.

This work was supported by a National Institutes of Health (NIH) predoctoral traineeship (GM07273, to E. A. Nothnagel), a Cornell graduate biophysics fellowship (to L. S. Barak), grants to W. W. Webb (NIH, GM21661B; National Science Foundation, 77-00311) and to J. W. Sanger (NIH, GM25653 and HL15835), and use of facilities of the Materials Science Center at Cornell.

Received for publication 7 August 1980, and in revised form 14 October 1980.

Note Added in Proof: It has recently been found that microinjected phalloidin does not inhibit axonal transport (Goldberg, D. J., D. A. Harris, B. W. Lubit, and J. H. Schwartz. Inhibition of axonal transport by proteins that depolymerize actin. *Proc. Natl. Acad. Sci. U. S. A.* In press.). We have recently found that perfusion with exogenous actin at 0.1 mg/ml strongly inhibits cytoplasmic streaming in *Chara* (Nothnagel et al., manuscript in preparation).

REFERENCES

1. Allen, N. S. 1974. Endoplasmic filaments generate the motive force for rotational streaming in *Nitella*. *J. Cell Biol.* 63:270–287.
2. Allen, N. S. 1976. Undulating filaments in *Nitella* endoplasm and motive force generation. *Cold Spring Harbor Conf. Cell Prolif.* 3(Book A):613–621.
3. Allen, N. S. 1980. Cytoplasmic streaming and transport in the characean alga *Nitella*. *Can. J. Bot.* 58:786–796.
4. Allen, N. S., and R. D. Allen. 1978. Cytoplasmic streaming in green plants. *Annu. Rev. Biophys. Bioeng.* 7:497–526.
5. Allen, R. D. 1977. Concluding remarks. *In* International Cell Biology. B. R. Brinkley and K. R. Porter, editors. Rockefeller University Press, New York. 403–406.
6. Barak, L. S., and R. R. Yocum. NBD-phallacidin: synthesis of a fluorescent actin probe. *Anal. Biochem.* In press.
7. Barak, L. S., R. R. Yocum, E. A. Nothnagel, and W. W. Webb. 1980. Fluorescence staining of the actin cytoskeleton in living cells with nitrobenzoxadiazole-phallacidin. *Proc. Natl. Acad. Sci. U. S. A.* 77:980–984.
8. Blatt, M. R., N. K. Wessells, and W. R. Briggs. 1980. Actin and cortical fiber reticulation in the siphonaceous alga *Vaucheria sessilis*. *Planta (Berl.)*. 147:363–375.
9. Bottomley, R. C., and I. P. Trayer. 1975. Affinity chromatography of immobilized actin and myosin. *Biochem. J.* 149:365–379.
10. Bradley, M. O. 1973. Microfilaments and cytoplasmic streaming: inhibition of streaming with cytochalasin. *J. Cell Sci.* 12:327–343.
11. Brenner, S. L., and E. D. Korn. 1979. Substoichiometric concentrations of cytochalasin D inhibit actin polymerization. *J. Biol. Chem.* 254:9982–9985.
12. Brown, S. S., and J. A. Spudich. 1979. Cytochalasin inhibits the rate of elongation of actin filament fragments. *J. Cell Biol.* 83:657–662.
13. Chen, J. C. W. 1973. Observations of protoplasmic behavior and motile protoplasmic fibrils in cytochalasin B-treated *Nitella* rhizoid. *Protoplasma.* 77:427–435.
14. Forsberg, C. 1965. Nutritional studies on *Chara* in axenic culture. *Physiol. Plant.* 18:275–290.
15. Hartwig, J. H., and T. P. Stossel. 1979. Cytochalasin B and the structure of actin gels. *J. Mol. Biol.* 134:539–553.
16. Kamitsubo, E. 1972. A "window technique" for detailed observation of characean cytoplasmic streaming. *Exp. Cell Res.* 74:613–616.
17. Kamiya, N., and K. Kuroda. 1956. Velocity distribution of the protoplasmic streaming *Nitella* cells. *Bot. Mag. Tokyo.* 69:544–554.
18. Kato, T., and Y. Tonomura. 1977. Identification of myosin in *Nitella flexilis*. *J. Biochem. (Tokyo).* 82:777–782.
19. Kersey, Y. M., P. K. Hepler, B. A. Palevitz, and N. K. Wessells. 1976. Polarity of actin filaments in characean algae. *Proc. Natl. Acad. Sci. U. S. A.* 73:165–167.
20. Kersey, Y. M., and N. K. Wessells. 1976. Localization of actin filaments in internodal cells of characean algae. *J. Cell Biol.* 68:264–275.
21. Korn, E. D. 1978. Biochemistry of actomyosin-dependent cell motility. *Proc. Natl. Acad. Sci. U. S. A.* 75:588–599.
22. Lin, D. C., K. D. Tobin, M. Grumet, and S. Lin. 1980. Cytochalasins inhibit nucleii-induced actin polymerization by blocking filament elongation. *J. Cell Biol.* 84:455–460.
23. Low, I., P. Dancker, and T. Wieland. 1975. Stabilization of F-actin by phalloidin reversal of the destabilizing effect of cytochalasin B. *FEBS (Fed. Eur. Biochem. Soc.) Lett.* 54:263–265.
24. Nagai, R., and T. Hayama. 1979. Ultrastructure of the endoplasmic factor responsible for cytoplasmic streaming in *Chara* internodal cells. *J. Cell Sci.* 36:121–136.
25. Nagai, R., and N. Kamiya. 1977. Differential treatment of *Chara* cells with cytochalasin B with special reference to its effect on cytoplasmic streaming. *Exp. Cell Res.* 108:231–237.
26. Nagai, R., and L. I. Rebhun. 1966. Cytoplasmic microfilaments in streaming *Nitella* cells. *J. Ultrastruct. Res.* 14:571–589.
27. Nothnagel, E. A., and W. W. Webb. 1979. Barrier filter for fluorescence microscopy of strongly autofluorescent plant tissues: application to actin cables in *Chara*. *J. Histochem. Cytochem.* 27:1000–1002.
28. Palevitz, B. A. 1980. Comparative effects of phalloidin and cytochalasin B on motility and morphogenesis in *Allium*. *Can. J. Bot.* 58:773–785.
29. Palevitz, B. A., and P. K. Hepler. 1975. Identification of actin *in situ* at the ectoplasm-endoplasm interface of *Nitella*. *J. Cell Biol.* 65:29–38.
30. Sanger, J. W. 1975. Changing patterns of actin localization during cell division. *Proc. Natl. Acad. Sci. U. S. A.* 72:1913–1916.
31. Sattelle, D. B., D. J. Green, and K. H. Langley. 1979. Subcellular motions in *Nitella flexilis* studied by photon correlation spectroscopy. *Physica Scripta.* 19:471–475.
32. Stockem, W., K. Weber, and J. Wehland. 1978. Influence of microinjected phalloidin on locomotion, protoplasmic streaming and cytoplasmic organization in *Amoeba proteus* and *Physarum polycephalum*. *Cytobiologie.* 18:114–131.
33. Tazawa, M., M. Kikuyama, and T. Shimmen. 1976. Electrical characteristics and cytoplasmic streaming of characean cells lacking tonoplast. *Cell Struct. Funct.* 1:165–176.
34. Weber, K., P. C. Rathke, M. Osborn, and W. W. Franke. 1976. Distribution of actin and tubulin in cells and in glycerinated cell models after treatment with cytochalasin B. *Exp. Cell Res.* 102:285–297.
35. Wehland, J., M. Osborn, and K. Weber. 1977. Phalloidin-induced actin polymerization in the cytoplasm of cultured cells interferes with cell locomotion and growth. *Proc. Natl. Acad. Sci. U. S. A.* 74:5613–5617.
36. Wehland, J., W. Stockem, and K. Weber. 1978. Cytoplasmic streaming in *Amoeba proteus* is inhibited by the actin-specific drug phalloidin. *Exp. Cell Res.* 115:451–454.
37. Wessells, N. K., B. S. Spooner, J. F. Ash, M. O. Bradley, M. A. Ludena, E. L. Taylor, J. T. Wrenn, and K. M. Yamada. 1971. Microfilaments in cellular and developmental processes. *Science (Wash. D.C.).* 171:135–143.
38. Wieland, T., and H. Faulstich. 1978. Amatoxins, phallotoxins, phallolysin and antamanide: the biologically active components of poisonous *Amanita* mushrooms. *Crit. Rev. Biochem.* 5:185–260.
39. Wieland, T., and V. M. Govindan. 1974. Phallotoxins bind to actins. *FEBS (Fed. Eur. Biochem. Soc.) Lett.* 46:351–353.
40. Williamson, R. E. 1972. A light-microscope study of the action of cytochalasin B on the cells and isolated cytoplasm of the characeae. *J. Cell Sci.* 10:811–819.
41. Williamson, R. E. 1975. Cytoplasmic streaming in *Chara*: a cell model activated by ATP and inhibited by cytochalasin B. *J. Cell Sci.* 17:655–668.
42. Williamson, R. E. 1976. Cytoplasmic streaming in characean algae. *In* Transport and Transfer Processes in Plants. I. F. Wardlaw and J. B. Passioura, editors. Academic Press, Inc., New York. 51–58.
43. Williamson, R. E. 1978. Cytochalasin B stabilizes subcortical actin bundles in *Chara* against a solution of low ionic strength. *Cytobiologie* 18:107–113.
44. Williamson, R. E. 1979. Filaments associated with the endoplasmic reticulum in the streaming cytoplasm of *Chara corallina*. *Eur. J. Cell Biol.* 20:177–183.
45. Williamson, R. E., and B. H. Toh. 1979. Motile models of plant cells and the immunofluorescent localization of actin in a motile *Chara* cell model. *In* Cell Motility: Molecules and Organization. S. Hatano, H. Ishikawa, and H. Sato, editors. University of Tokyo Press, Tokyo. 339–346.
46. Yocum, R. R. 1978. New laboratory scale purification of β-amanitin from American *Amanita phalloides*. *Biochemistry.* 17:3786–3789.